

Supporting Information

Personal Exposure to PM_{2.5} Black Carbon and Aerosol Oxidative Potential using an Automated Microenvironmental Aerosol Sampler (AMAS)

*Casey Quinn†, Daniel D. Miller-Lionberg‡, Kevin J. Klunder§, Jaymin Kwon||, Elizabeth M.
Noth⊥, John Mehaffy‡, David Leith‡Δ, Sheryl Magzamen†, S Katharine Hammond⊥, Charles
S. Henry*§, and John Volckens*†‡*

†Department of Environmental and Radiological Health Sciences, Colorado State University,
Fort Collins, Colorado 80523, USA; ‡Department of Mechanical Engineering, Colorado State
University, Fort Collins, Colorado 80523, USA; §Department of Chemistry, Colorado State
University, Fort Collins, Colorado 80523, USA; ||Department of Public Health, California State
University, Fresno, California 93740, USA; ⊥Division of Environmental Health Sciences,
University of California, Berkeley, Berkeley, California 94720, USA; Δ Department of
Environmental Sciences and Engineering, University of North Carolina at Chapel Hill, Chapel
Hill, NC, 27599, USA

**Corresponding Authors:*

Phone: 1-970-491-6341. E-mail: john.volckens@colostate.edu (J.V.).

Phone: 1-970-491-2852. E-mail: chuck.henry@colostate.edu (C.S.H.).

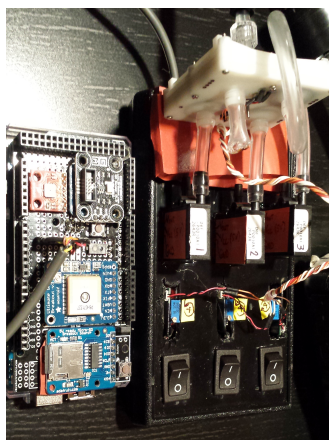
Supporting information (30 pages) contains 19 figures, 9 equations, 1 table, and 1 method.

Table of Contents

Figure S1: AMAS Evolution.....	S4
Figure S2: Cyclone Performance.....	S5
Figure S3: Phone Application Screenshots.....	S6
Figure S4: Traditional personal sampler (Reference) equipment.....	S7
Figure S5: Custom Sootscan 15mm Holder.....	S8
Figure S6: Microenvironment Transition Distance.....	S9
Figure S7: Black Carbon Concentrations.....	S10
Figure S8: Oxidative Potential Concentrations.....	S11
Figure S9: Oxidative Potential Measurement Uncertainty.....	S12
Figure S10: Black Carbon Deming Regression.....	S13
Figure S11: Black Carbon Bland-Altman Plot.....	S14
Figure S12: Collocated Black Carbon Comparison.....	S15
Figure S13: Collocated Black Carbon Concentration Comparison.....	S16
Figure S14: Oxidative Potential Deming Regression.....	S17
Figure S15: Oxidative Potential Bland-Altman Plot.....	S18

Figure S16: Black Carbon Comparison	S19
Figure S17: Black Carbon Concentration Map.....	S20
Figure S18: Black Carbon Ratio Comparison	S21
Figure S19: Participant Survey Summary.....	S22
Equation S1: Black Carbon Mass	S23
Equation S2: Black Carbon Mass Concentration	S23
Equation S3: Inhaled Black Carbon Mass.....	S23
Equation S4: Cumulative AMAS Black Carbon Concentration	S23
Equation S5: DTT Concentration.....	S24
Equation S6: Oxidative Potential.....	S24
Equation S7: Oxidative Potential Per Sampled Air Volume.....	S24
Equation S8: Inhaled Oxidative Potential.....	S24
Equation S9: Cumulative AMAS Oxidative Potential.....	S25
Table S1: AMAS Sensor Components and Electronics.....	S26
Experimental DTT Method.....	S27
References.....	S30

Proof of Concept



Prototype



1st Gen



2nd Gen



Figure S1: AMAS evolution. The AMAS originated as a proof of concept consisting of an Arduino with breakout boards (light sensing, GPS, SD card, temperature, pressure, and relative humidity), three Omron flow sensors, three manual toggle valves, a rapid prototype filter holder, and a SKC personal air sampler. Following the proof of concept, the inlet of an Ultrasonic Personal Aerosol Sampler (UPAS)¹ was modified to include four separate filter-valve flow channels with custom valves that were controlled by the UPAS microcontroller. After testing with the prototype, two generations of the PM_{2.5} inlets have been developed to date. Similar to the prototype, the first generation consisted of four individual plastic filter cartridges that fit into a separate PM_{2.5} cyclone inlet. The second generation replaced the individual filter cartridges with a single aluminum filter holder which holds all four filters. Additionally, the second-generation inlet integrated the cyclone inlets into a single inlet/cover to make the device more aesthetically pleasing. The second-generation AMAS also contains a multidirectional inlet to reduce the possibility of blocked air flow, which was a concern in the first-generation design. Cyclone designs have been developed for 1.0, 1.5, and 2.0 Lmin⁻¹ operation and can be easily integrated into the AMAS design. The first-generation AMAS used four 2.0 Lmin⁻¹ cyclones, and the second-generation AMAS used four 1.5 Lmin⁻¹ cyclones; however, AMAS the inlet can be designed to incorporate a combination of 1.0, 1.5, and 2.0 min⁻¹ cyclone design.

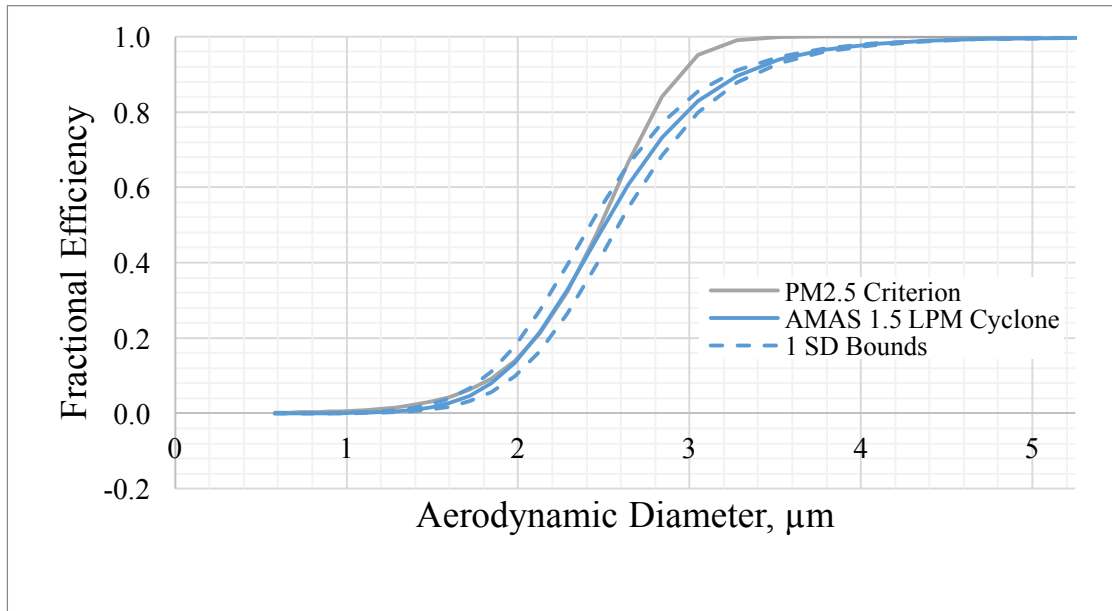


Figure S2: Cyclone performance. Collection efficiency for the 1.5 Lmin⁻¹ cyclone design used in this study. The cyclone design was developed with the same methods detailed by Volckens et. al.¹ and use cyclone dimension nomenclature defined by Kenny and Gussman.^{2,3} The cyclone dimensions in mm are as follows; $D_c=9.43$, $D_m=2.212$, $D_e=2.546$, $B=2.358$, $H=4.055$, $Z=10.657$, $S=3.301$. Laboratory testing of the cyclone provided a d_{50} (50% collection efficiency) of particles with an aerodynamic diameter of $2.5\mu\text{m}$ of 2.50 ± 0.08 and a β (slope parameter) of 7.98 ± 0.34 where the confidence intervals are one standard deviation.

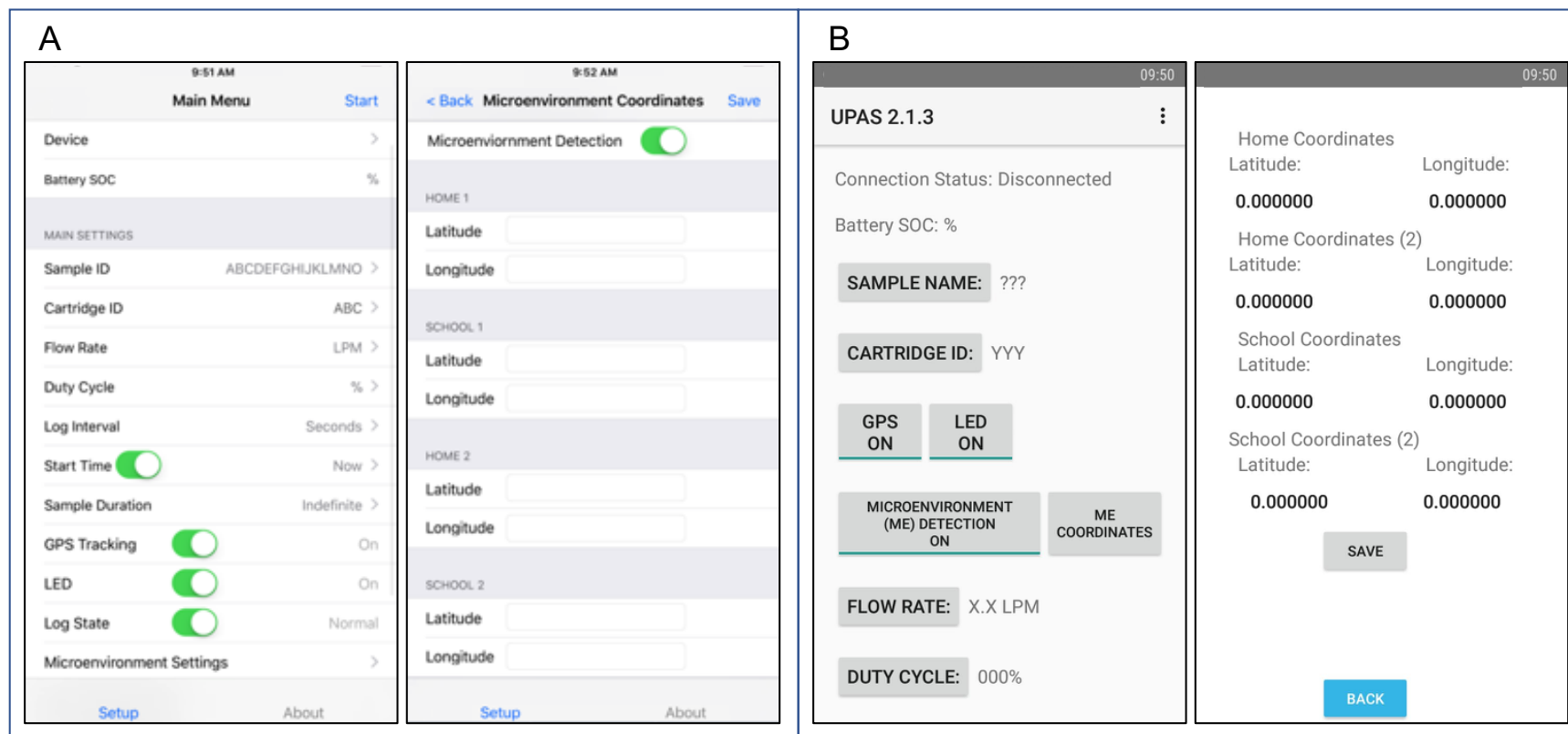


Figure S3: Phone application screenshots. A) iOS, B) Android.

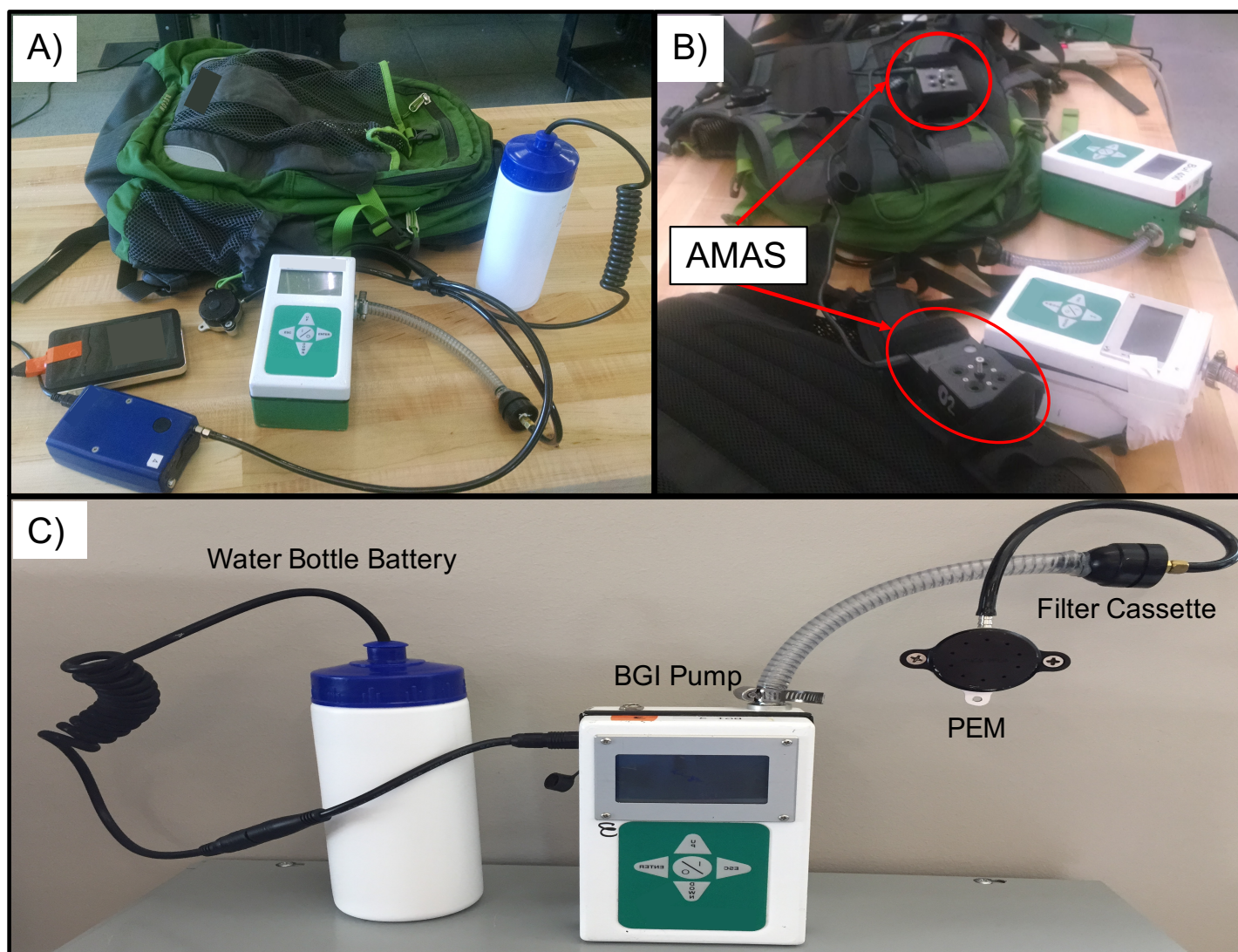


Figure S4: Traditional personal sampler (Reference) equipment.

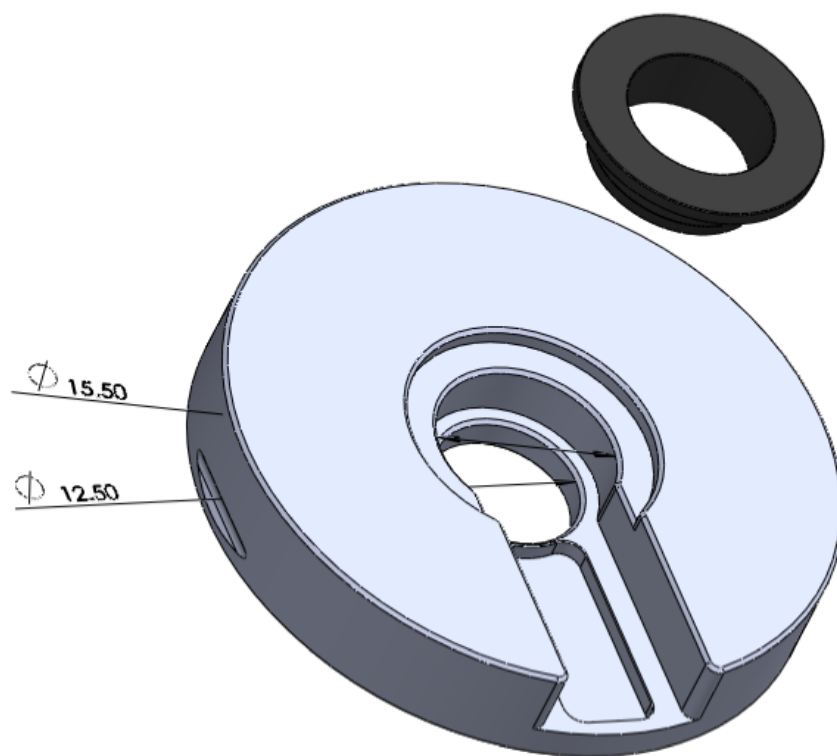


Figure S5: Custom 15mm Sootscan filter holder. Anodized aluminum lower filter holder with a 12.5 mm view diameter hole (identical to the standard 25 mm Magee Scientific Sootscan filter holder) and a 15.5 mm cavity to accommodate 15 mm filters. A plastic insert for securing the filter is also shown and has a 12.5 mm through hole as well.

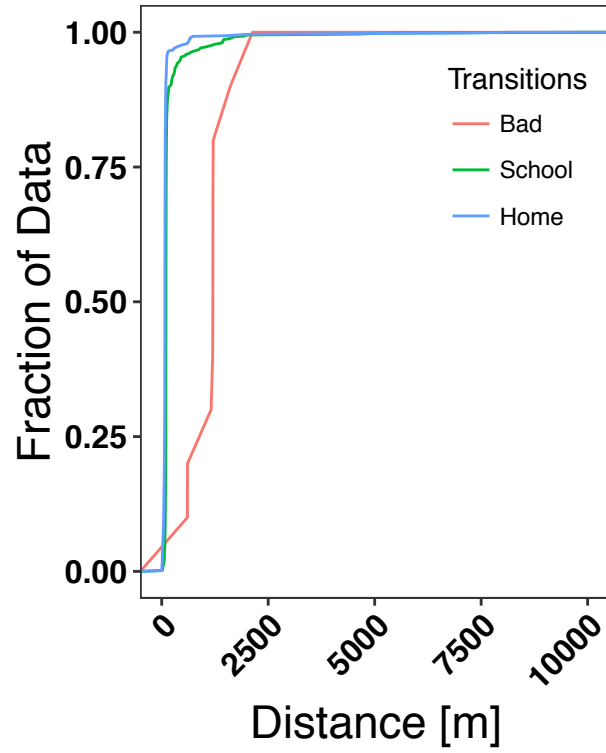


Figure S6: Microenvironment transition distance. The cumulative distributions for the distance from a microenvironment at the time of a transition for both entering and exiting the home and school microenvironments (Bad, $n = 10$; School, $n = 585$; Home, $n = 780$). Bad is defined as a transition that occurs between a school and a home microenvironment without detecting time in the other microenvironment.

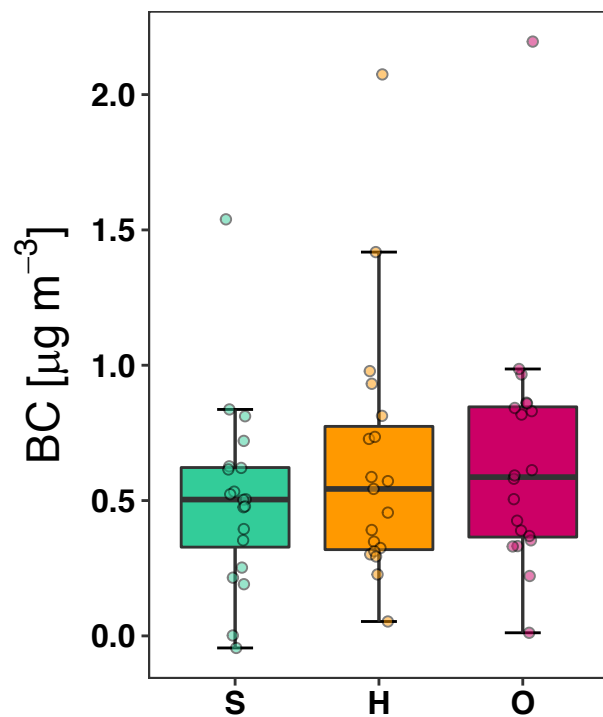


Figure S7: Black carbon concentrations. The data shown in the plots include only samples that collected $\text{PM}_{2.5}$ and AMAS data for the entire 48-hr period, had valid GPS coordinates, and collected $\text{PM}_{2.5}$ for more than an hour (0.1 m^3) in each microenvironment. ($n = 20, 19, 20$ for S = school, H = home, and O = other).

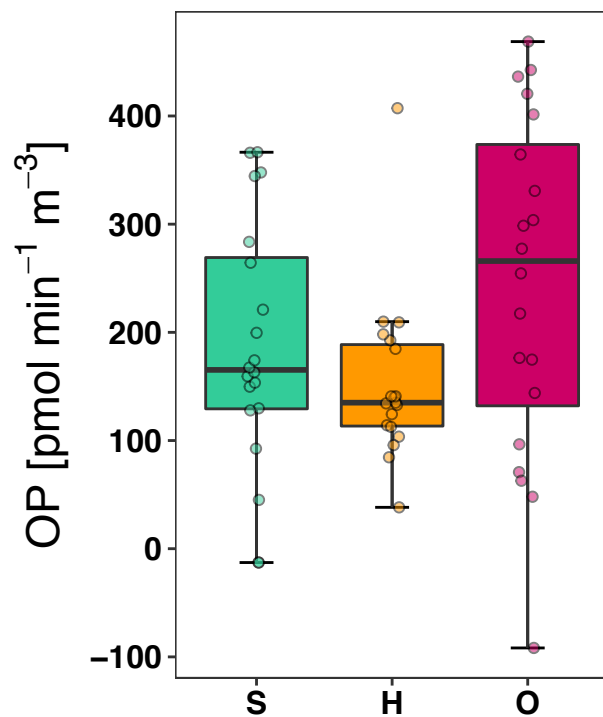


Figure S8: Oxidative potential concentrations. The data shown in the plots only include samples which collected $\text{PM}_{2.5}$ and AMAS data for the entire 48-hr period, had valid GPS coordinates, and collected $\text{PM}_{2.5}$ for more than an hour (0.1 m^3) in each ME ($n = 20, 19, 20$ for $S = \text{school}$, $H = \text{home}$, and $O = \text{other}$).

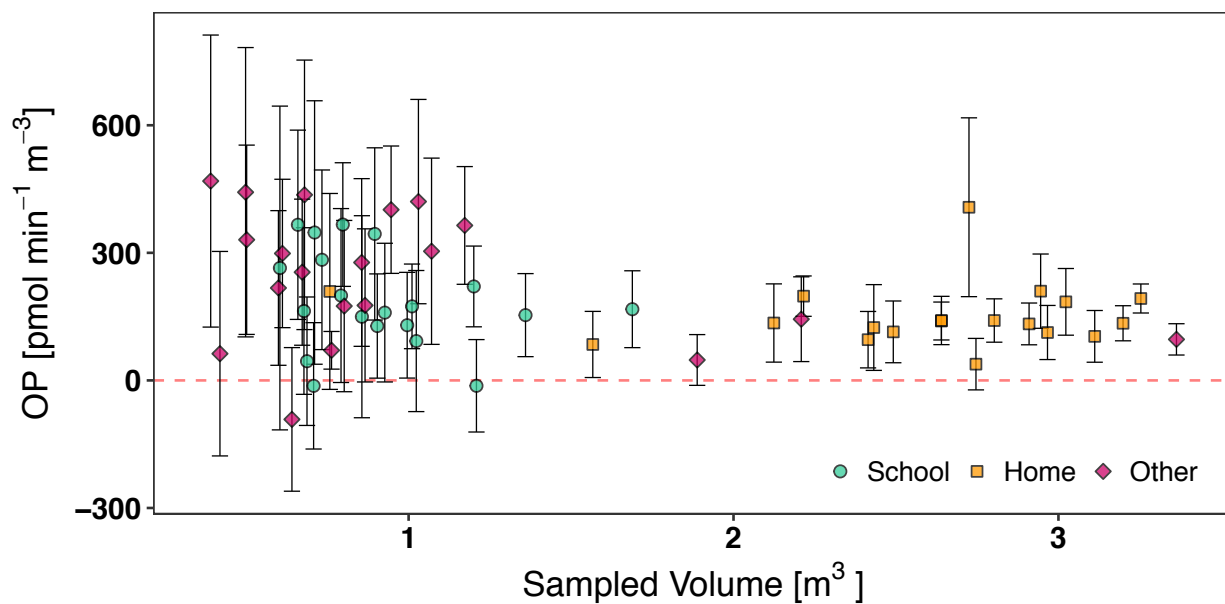


Figure S9: Oxidative potential measurement uncertainty. The data shown in the plots only include filter samples that collected $\text{PM}_{2.5}$ and AMAS data for the entire 48-hr period, had valid GPS coordinates, and collected $\text{PM}_{2.5}$ for more than an hour (0.1 m^3) in each microenvironment ($n = 20, 19, 20$ for S = school, H = home, and O = other).

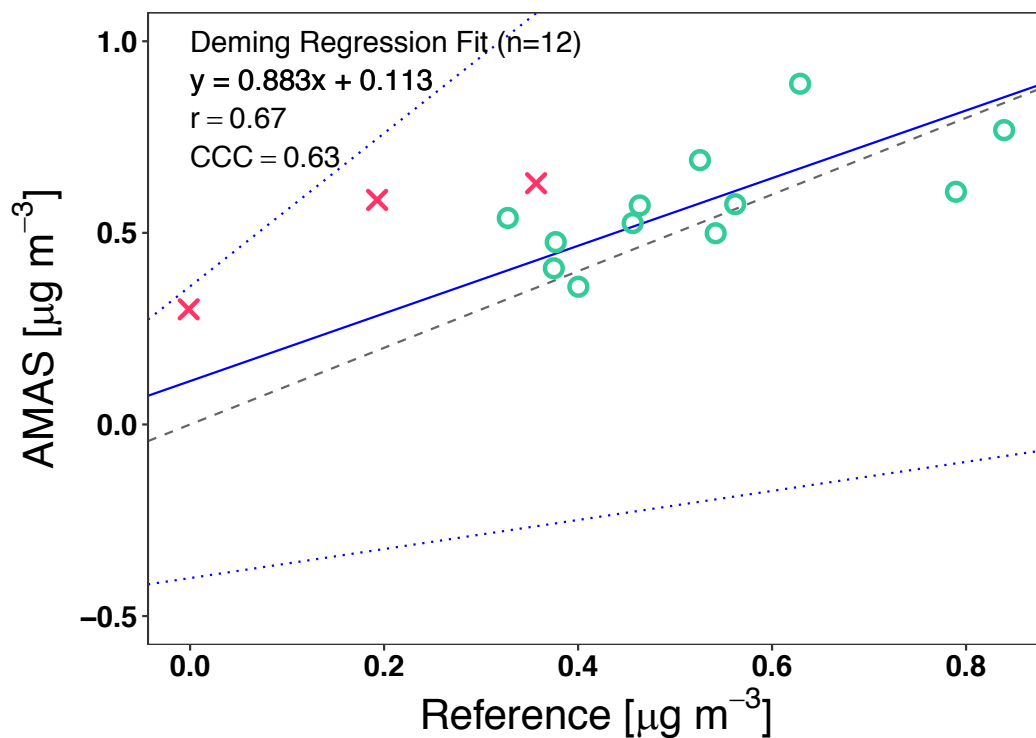


Figure S10: Black carbon Deming regression. Comparison of the cumulative AMAS filter BC concentration to that of the BC concentrations measured by the traditional personal sampler used for reference. A Deming regression was used to compare 12 of the 15 samples (green circles). The three samples when the traditional personal sampler had malfunctions (red multiplication signs) were excluded from the regression. The Deming regression (solid blue line) had a slope of 0.88 (0.37, 1.97) and an intercept of 0.11 (-0.39, 0.37). The 95% confidence intervals (dotted blue lines) and the 1:1 line (dashed gray line) are also shown in the figure.

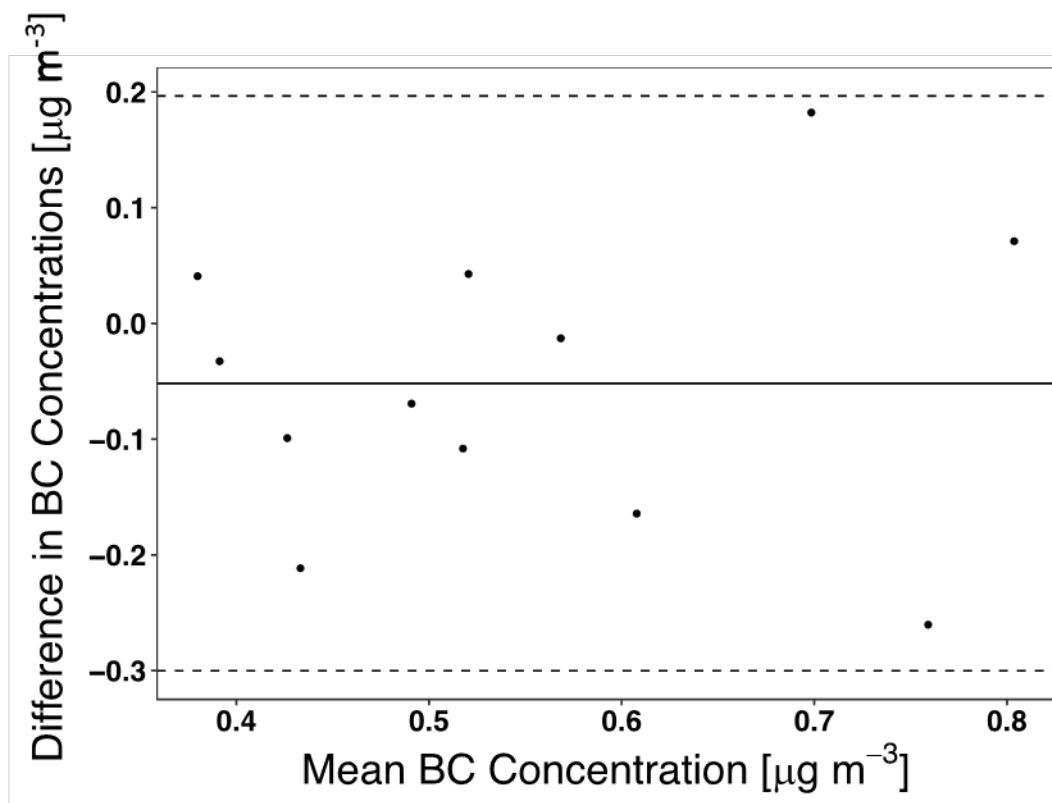


Figure S11: Black carbon Bland-Altman plot. Comparison of the cumulative AMAS filter BC concentration to that of the BC concentrations measured by the traditional personal sampler used for reference. A Bland-Altman analysis was used to compare 12 of the 15 samples. The three samples when the traditional personal sampler had malfunctions were excluded from the analysis. The limits of agreement are shown by the black dashed lines at -0.30 and $0.20 \mu\text{g m}^{-3}$.

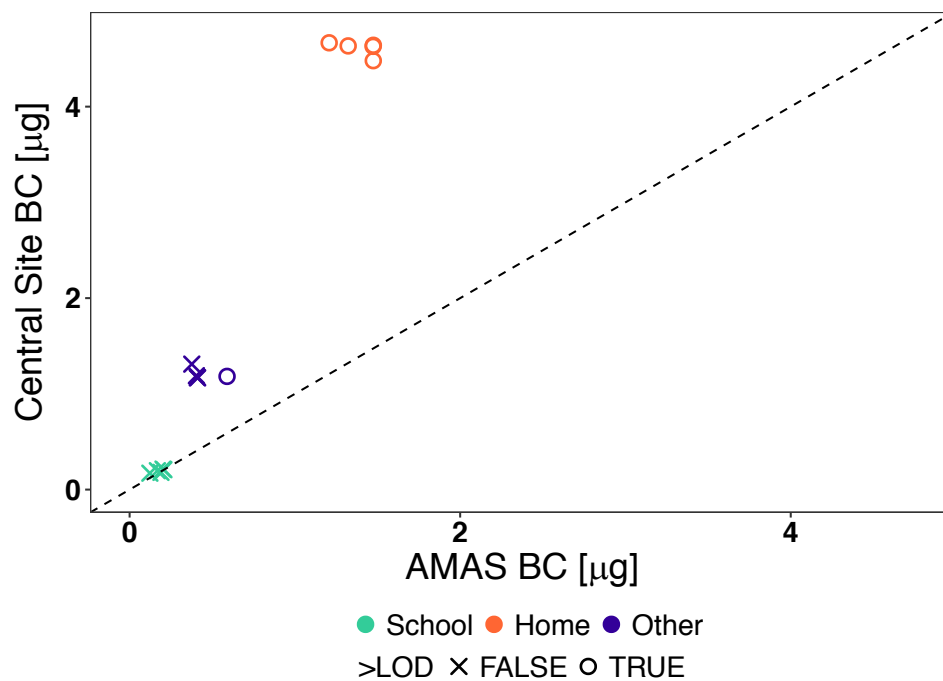


Figure S12: BC mass comparisons of AMAS collocation monitors to AE33.

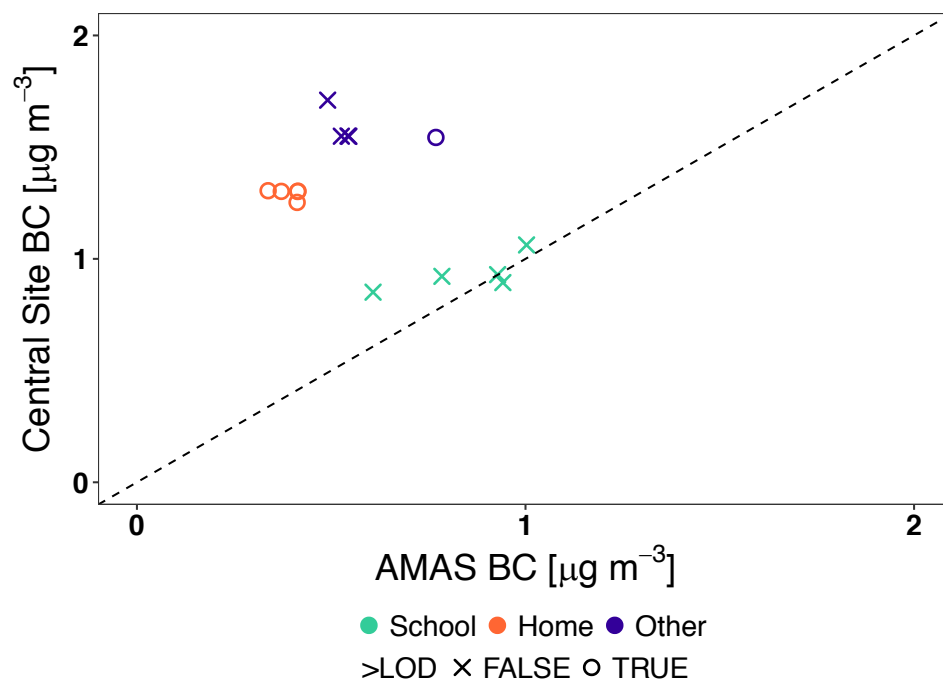


Figure S13: BC concentration comparisons of AMAS collocation monitors to AE33.

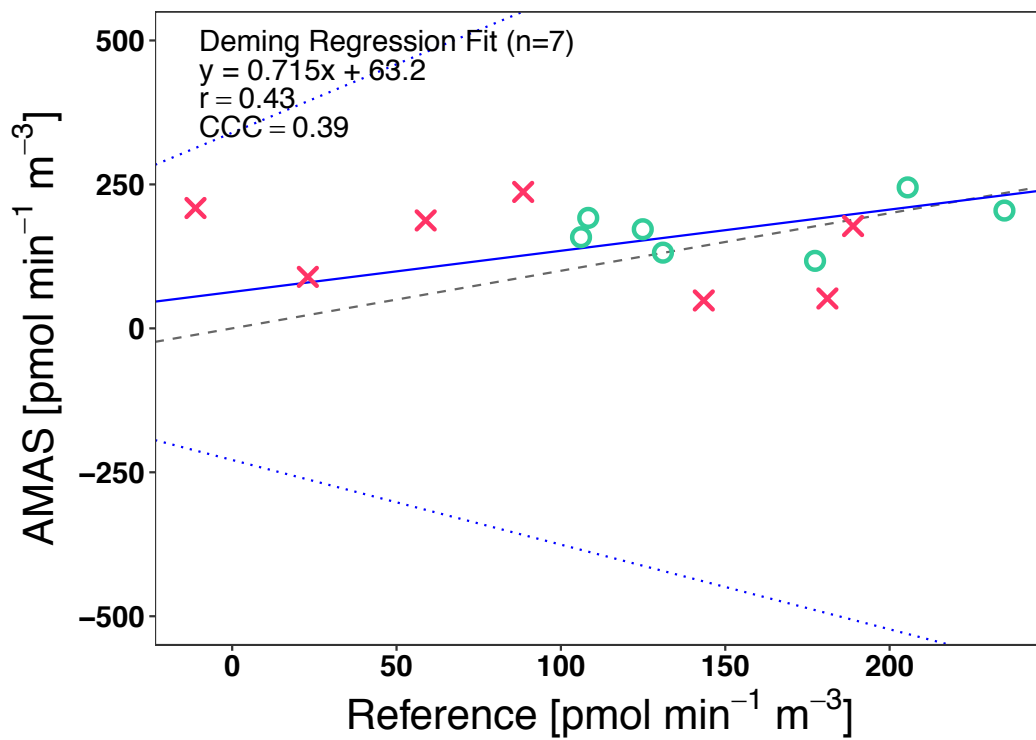


Figure S14: Deming regression of AMAS and reference sampler OP. Comparison of the cumulative AMAS filter OP measured using the dithiothreitol (DTT) assay to that of the paired traditional personal sampler OP. The regression was evaluated using 7 of the 15 samples (green circles). The three samples when the traditional personal sampler had malfunctions and the five samples that had an OP less than 100 $\text{pmol min}^{-1} \text{m}^{-3}$ (red multiplication signs) were excluded from the regression. The values less than 100 $\text{pmol min}^{-1} \text{m}^{-3}$ were excluded due to the uncertainty of the assay when the reactivity of the sample was low. The Deming regression (solid blue line) had a slope of 0.67 (-0.99, 2.6) and an intercept of 69 (-270, 290). The 95% confidence intervals (dotted blue lines) and the 1:1 line (dashed gray line) are also shown in the figure.

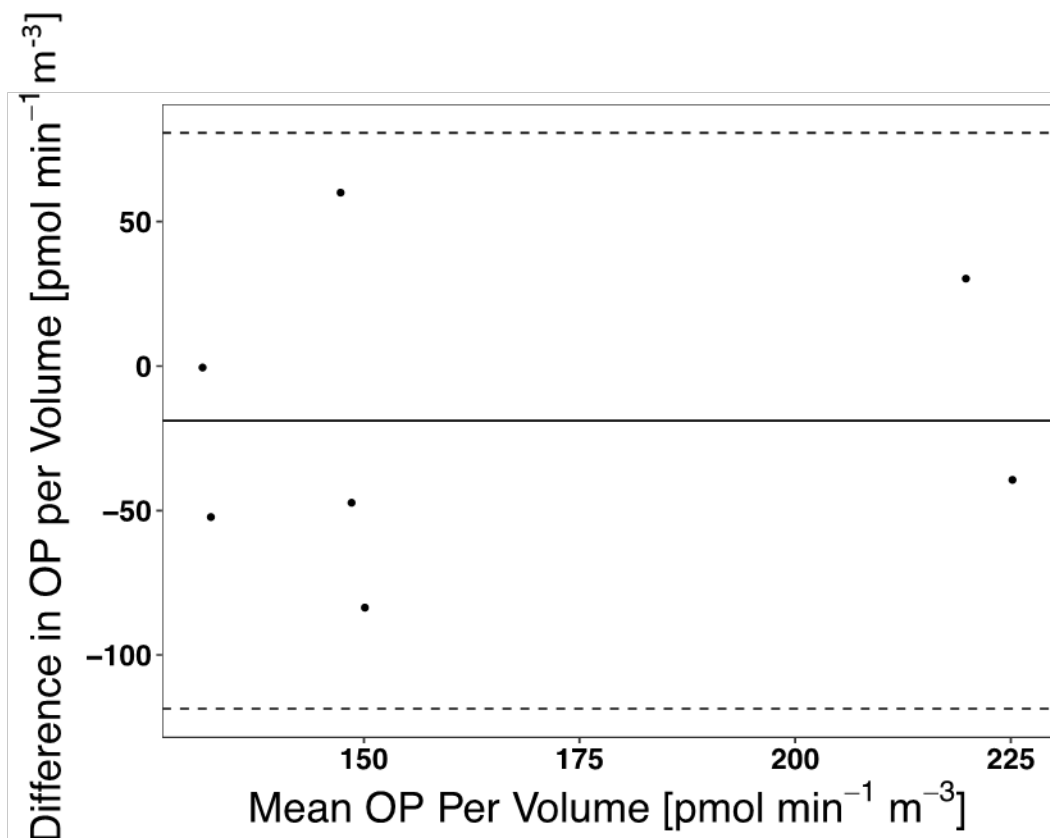


Figure S15: Bland-Altman analysis of AMAS and reference sampler OP. Comparison of the cumulative AMAS filter OP measured using the dithiothreitol (DTT) assay to that of the paired traditional personal sampler OP. A Bland-Altman analysis was used to compare 7 of the 15 samples. The three samples when the traditional personal sampler had malfunctions or the OP was less than 100 pmol min⁻¹ m⁻³ were excluded from the regression. The values less than 100 pmol min⁻¹ m⁻³ were excluded due to the uncertainty of the assay when the reactivity of the sample was low. The limits of agreement are shown by the black dashed lines at -119 and 81 pmol min⁻¹ m⁻³.

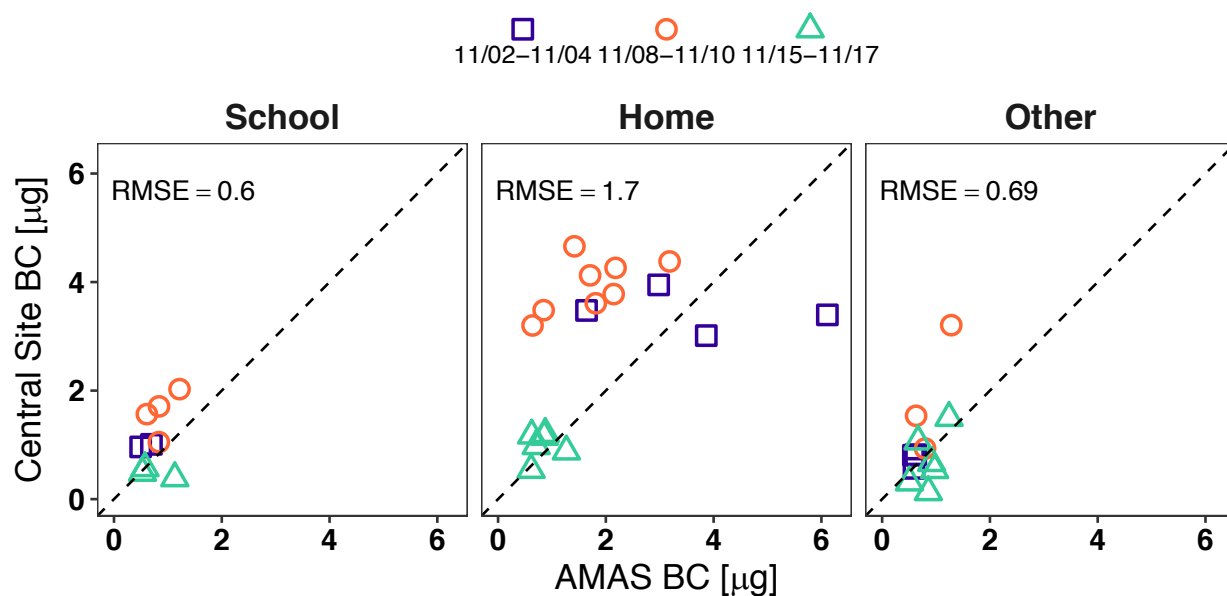


Figure S16: Central site BC mass compared to AMAS filter BC mass by microenvironment. The data shown in the plots only include samples which collected PM_{2.5} and AMAS data for the entire 48-hr period, had valid GPS coordinates, collected PM_{2.5} for more than an hour (0.1 m³) in each ME, and the BC measurement was above the LOD (0.49 μg) of the Magee Scientific Sootscan measurement (School, n = 9; Home, n = 18; Other, n = 12). The root mean square error (RMSE) is shown in each microenvironment panel.

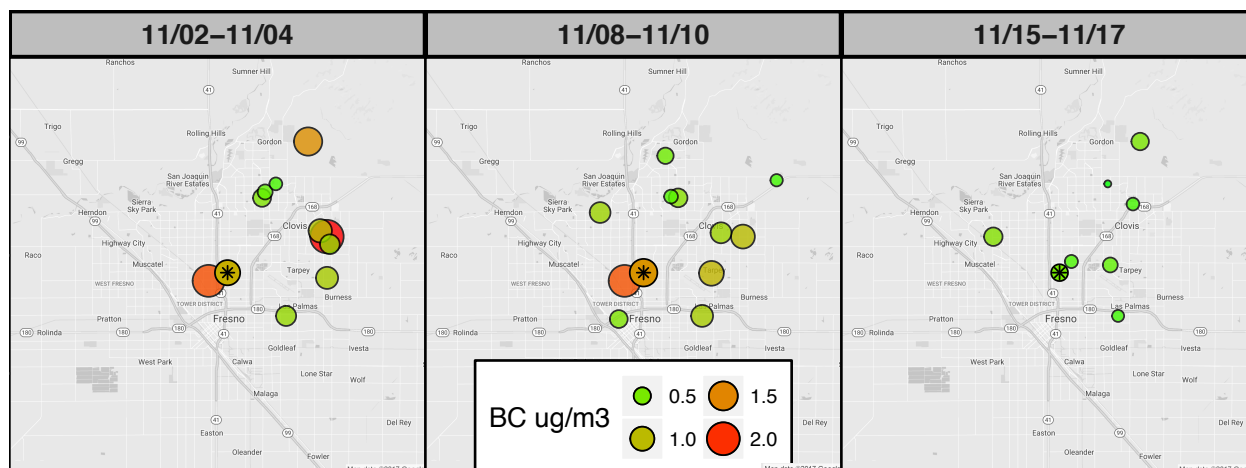


Figure S17: BC concentration spatial distribution. Home microenvironment concentrations and AE33 48-hour concentration (denoted with a "*") for the three 48-hour sampling periods.

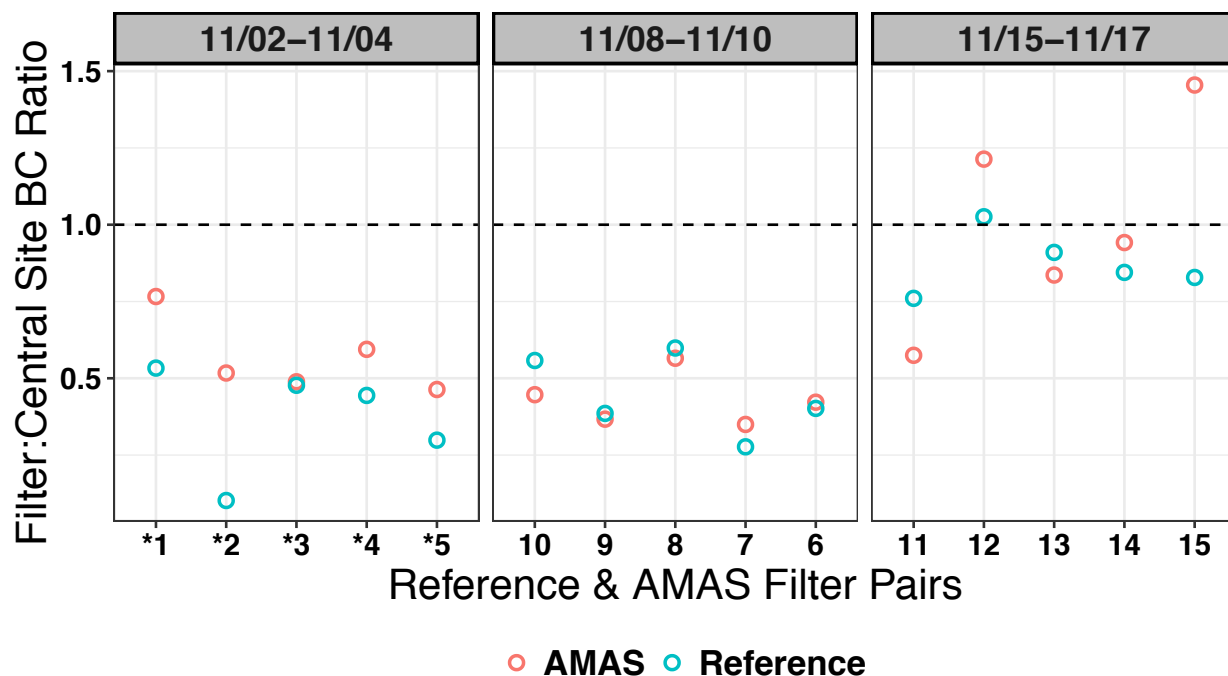


Figure S18: BC comparisons of the reference sampler-AMAS paired data to AE33. This demonstrates that both the traditional personal sampler and AMAS show some bias as compared to the AE33 measurements on high BC days, but not low BC days (11/15-11/17). The estimates come from using the hourly data for the AE33 to calculate the amount of mass expected compared to the mass found with the Magee Scientific Sootscan analysis.

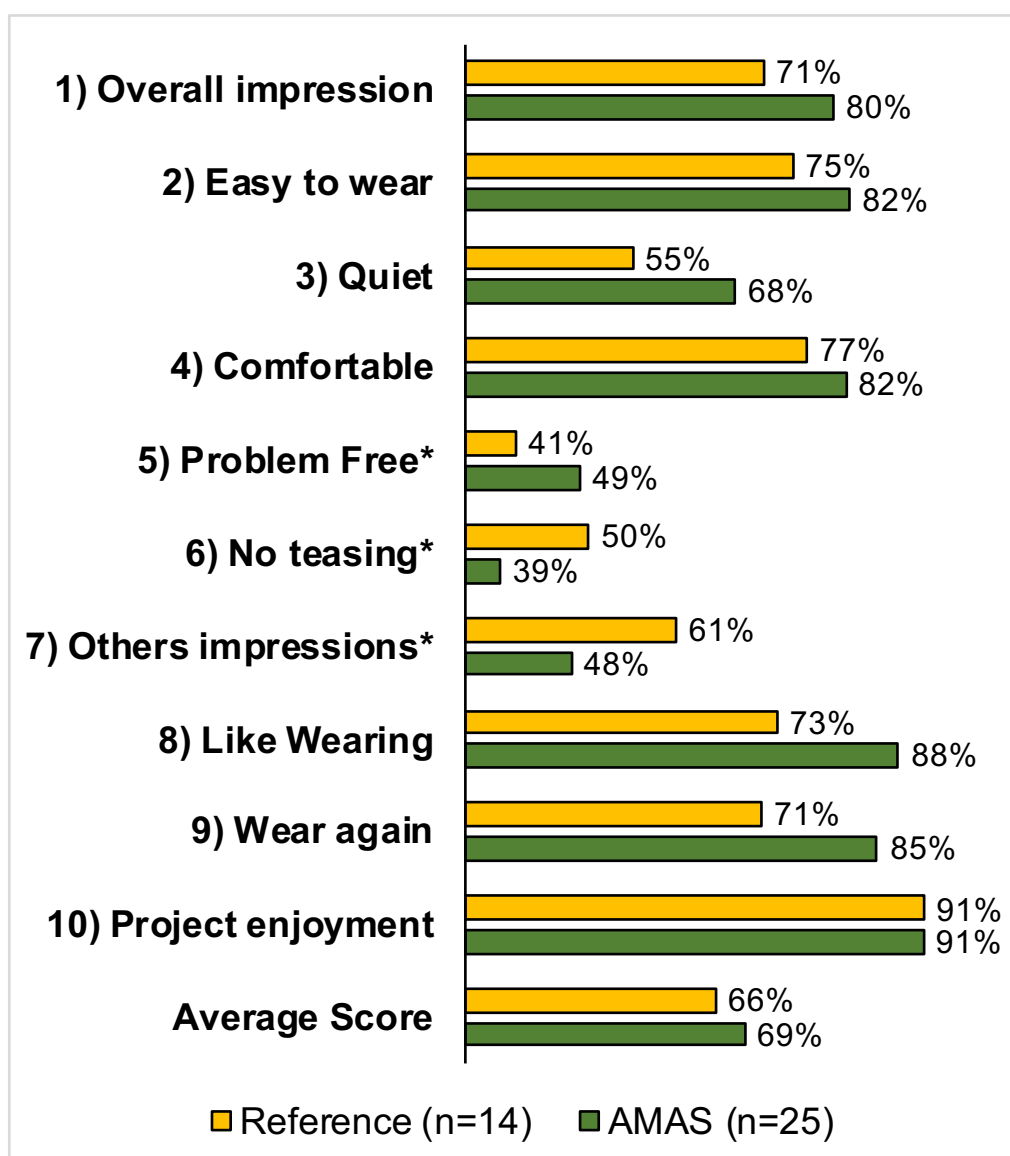


Figure S19: Participant survey summary. Summarized results from the survey's taken by the participants after their 48-hour sample collection period. Each participant was asked to take a survey only once even if they participated in more than one 48-hour sample period. Participants who carried both an AMAS and a traditional personal sampler for reference were asked to take the survey for the reference monitor in addition to the AMAS survey. Blank questionnaires are also provided with the supplemental information for reference. The numbers correspond to the questions in each survey and questions 5, 6, and 7 are marked with an astrix to denote that problematic wording was used in the survey that led to issues with computing the Average Score.

$$BC_{\mu g} = \left(\frac{100 * \ln \left(\frac{IR_{PRE}}{IR_{POST}} \right)}{\sigma_{ATN}} \right) * Area_{Filter}$$

Equation S1: Black carbon mass.

IR_{PRE}: Infrared filter transmitted intensity pre-sample

IR_{POST}: Infrared filter transmitted intensity post-sample

σ_{ATN}: Mass absorption cross-sections (cm² μg⁻¹)

Area_{Filter}: Active filter area (cm²):

15 mm: 13.2 cm²; 25 mm Teflon: 3.50 cm²; 25 mm FiberfilmTM: 3.66 cm²

$$BC_{\frac{\mu g}{m^3}} = \left(\frac{BC_{\mu g}}{Vol} \right)$$

Equation S2: Black carbon mass concentration.

Vol: Sampled volume recorded for that filter (m³)

$$Inhaled BC_{\mu g \text{ day}^{-1}} = \frac{Inhalation Rate * BC_{\frac{\mu g}{m^3}} * Time_{ME}}{Total Sample Duration}$$

Equation S3: Inhaled black carbon mass.

Inhalation Rate: Long-term exposure inhalation rate (m³ day⁻¹)

Time_{ME}: Microenvironment sample time (day)

Total Sample Duration: Total sample period (day)

$$\Sigma AMAS BC_{\frac{\mu g}{m^3}} = \left(\frac{School BC_{\mu g} + Home BC_{\mu g} + Other BC_{\mu g}}{Vol_{School} + Vol_{Home} Vol_{Other}} \right)$$

Equation S4: Cumulative AMAS BC concentration.

$$[DTT]_{\mu M} = \left(\frac{\left(\frac{TNB \text{ abs.}}{14150 \frac{mole}{liter}} \right) * 5(dilution)}{\frac{2 \text{ moles } TNB}{1 \text{ mole } DTT}} \right) * 1000000 \frac{\mu L}{L}$$

Equation S5: DTT concentration.

abs: UV-Vis absorbance;

$$OP_{\mu M \text{ min}^{-1}} = -1 * \left(\left(\frac{\Delta[DTT]}{\Delta t} \right) - BFC \right) * Ff$$

Equation S6: Oxidative potential.

$\Delta [DTT]$: Change in [DTT]

Δt : Elapsed time for all [DTT] measurements (min)

BFC: Blank filter correction ($\mu M \text{ min}^{-1}$)

Ff: Fraction of filter used for OP analysis (-)

Note: $\left(\frac{\Delta[DTT]}{\Delta t} \right)$ was calculated using the LINEST() function in MS Excel.

$$OP_{pmol \text{ min}^{-1} m^{-3}} = \left(\frac{OP_{\mu M \text{ min}^{-1}} * Vol_{assay}}{Vol_{air}} \right)$$

Equation S7: Oxidative potential per sampled air volume.

Vol_{assay} : DTT assay volume (μL)

Vol_{air} : Sampled volume recorded for that filter (m^3)

$$Inhaled \text{ } OP_{(\mu M \text{ min}^{-1}) \text{ day}^{-1}} = \frac{Inhalation \text{ Rate} * \left(\frac{OP_{\mu M \text{ min}^{-1}}}{Vol} \right) * Time_{ME}}{Total \text{ Sample Duration}}$$

Equation S8: Inhaled oxidative potential.

Inhalation Rate: Long-term exposure inhalation rate ($m^3 \text{ day}^{-1}$)

$Time_{ME}$: Microenvironment sample time (day)

Total Sample Duration: Total sample period (day)

$$\Sigma AMAS\ OP\ \frac{pmol}{min*m^3} = \left(\frac{(School\ OP_{\mu M\ min^{-1}} + Home\ OP_{\mu M\ min^{-1}} + Other\ OP_{\mu M\ min^{-1}}) * Vol_{assay}}{Vol_{School} + Vol_{Home} + Vol_{Other}} \right)$$

Equation S9: Cumulative AMAS OP per sampled air volume.

Table S1: AMAS Sensor Components and Electronics.

Component	Manufacturer	Part Number
Microblower	Murata	MZBD001
Mass Air Flow Sensor	Honeywell	Omron D6F
Light Sensor (vis., UV, IR)	Silicon Labs	SI1145-A10-GMR
Temp., Pressure, RH Sensor	Bosch Sensortec	BME280
Accelerometer/Magnetometer	STMicroelectronics	LSM303DLHCTR
Bluetooth Low-Energy	Microchip	RN4677
MicroSD Card	Molex	5031821852
Memory (EEPROM)	Atmel	AT24CM01-XHM-T
Real-time Clock	Maxim Integrated	DS3231MZ+
Battery (2800 mAh)	Samsung	SAEBBG900BBU
Global Positioning System	Ublox	CAM-M8Q
Valve Manifold	Custom	N/A
Valve Manifold Gear Motor	Precision Microdrive	206-108

Experimental DTT Method

Chemicals and materials. Ultrapure water (18.2 MΩcm) from a Mill-Q system was used for the preparation of solutions and cleaning of supplies and equipment (Merck Millipore, Darmstadt, Germany). Phosphoric acid (EMD), potassium phosphate monobasic 100.1% purity (Sigma), potassium phosphate dibasic 100.1% purity (Baker), dithiothreitol (DTT) (Acros), Ellman's reagent(DTNB) 5,5'-dithiobis-(2-nitrobenzoic acid) (Pierce), 2,2,2-Trifluoroethanol (Sigma), Chelex® 200-400 mesh sodium form (BIO-RAD).

Stock solutions. Stock solutions were 0.001 M phosphoric acid with a concentration of 4.5 mM of DTT. The dilute acid stabilizes the DTT and enables the stock solution to be used through a day of testing. DTT 4.5 mM stock solutions were remade fresh after 24 hours. DTNB was a stock solution of ~56 μM in 0.1 M phosphate buffer at pH of ~7.5. The DTNB was stable for 2 about months with storage in a 3°C refrigerator.

Chelex treatment. As a one-time pretreatment, the Chelex was washed with 3 liters of deionized water to remove any slightly soluble Chelex moieties, and then treated with washing (a few liters) with high purity 0.1 M phosphate buffer to adjust to pH to 7.4. To make buffer solution for use in the DTT assay, high purity potassium dibasic and monobasic phosphate buffer was made into 0.1 M individual solutions. The solutions were then combined incrementally until a pH of 7.4 was reached. Roughly 200 mL of the pH 7.4 phosphate solution was then added to ~50 grams of the pretreated Chelex in a Nalgene bottle, which was shaken periodically for a period of 1 to 3 weeks while being stored in a 3 °C refrigerator. After the 1 to 3 week time period, the buffer solution was decanted into a plastic syringe and filtered through a 0.22 μm PVDF filter (CELLTREAT). The filtered Chelex treated buffer was then stored in a Nalgene container and typically used within a few weeks.

DTT Assay protocol: The 15 mm filters were cut in half and the 25 mm filters were quartered with ceramic scissors; one filter half or quarter was used for the DTT assay. The DTT assay was performed similar to the traditional method⁴; however, quenching with acid was not necessary as the samples were run immediately after DTNB addition, eliminating two pipetting/dilution steps in the process. The reaction of DTNB and DTT is near instantaneous at pH ~7.5, and we found a 1.5 molar excess (3 moles DTNB: 1 moles DTT) was sufficient for quenching, this then prevents the UV-Vis peak from DTNB interfering with the TNB peak at 412 nm.

To run the DTT assay, filters were placed in 1.5 mL centrifuge tubes (Eppendorf) and wet with 15 μ L of 50/50 2,2,2-trifluoroethanol and MilliPore water. Trifluoroethanol has been reported to aid in wetting the surface of the filter and has been used previously in similar studies.⁵ 500 μ L of buffered 75 μ M DTT solution was then added to the vials, which was made fresh minutes before running the assay. Stock 0.001 M phosphoric acid with a concentration of 4.5 mM of DTT, diluted by the Chelex buffer, was used to make the 75 μ M DTT solution. The dilute acid stabilizes the DTT and enables the stock 4.5 mM DTT solution to be used through a day of testing, these solutions were remade fresh after 24 hours.

The vials were placed in a 37 °C water bath. At time points 0, ~15, ~30, and ~45 minutes 100 μ L aliquots were removed from the vials and added to 400 μ L of stock DTNB solution. The DTNB concentration was ~56 μ M in 0.1 M phosphate buffer at pH of ~7.5. Spectra were measured four times (0, 15, 30, and 45 minutes) with a UV-Vis spectrophotometer (Agilent 8453, Santa Clara, CA, USA) within ~15 minutes of reacting DTT with DTNB. The absorbance at 412 nm was used to measure TNB concentration. The concentration was calculated with Beer's law using a molar extinction coefficient of 14150 M⁻¹ cm⁻². For all trials two blank DTT decay rates were measured,

blank rates were also recorded in the presence on non-PM loaded filters as a control for any filter related activity.

References

1. Volckens, J.; Quinn, C.; Leith, D.; Mehaffy, J.; Henry, C. S.; Miller-Lionberg, D., Development and evaluation of an ultrasonic personal aerosol sampler. *Indoor air* **2017**, 27 (2), 409-416.
2. Kenny, L.; Gussman, R., A direct approach to the design of cyclones for aerosol-monitoring applications. *Journal of aerosol science* **2000**, 31 (12), 1407-1420.
3. Kenny, L.; Gussman, R.; Meyer, M., Development of a sharp-cut cyclone for ambient aerosol monitoring applications. *Aerosol Science & Technology* **2000**, 32 (4), 338-358.
4. Cho, A. K.; Sioutas, C.; Miguel, A. H.; Kumagai, Y.; Schmitz, D. A.; Singh, M.; Eiguren-Fernandez, A.; Froines, J. R., Redox activity of airborne particulate matter at different sites in the Los Angeles Basin. *Environmental Research* **2005**, 99 (1), 40-47.
5. Charrier, J. G.; McFall, A. S.; Vu, K. K.; Baroi, J.; Olea, C.; Hasson, A.; Anastasio, C., A bias in the “mass-normalized” DTT response—An effect of non-linear concentration-response curves for copper and manganese. *Atmospheric Environment* **2016**, 144, 325-334.